POWERING CONCEPTS FOR RESISTIVE MAGNETS IN THE MUON COLLIDER RAPID CYCLING SYNCHROTRON*

F. Boattini†, D. Aguglia, L. Bottura
European Organization for Nuclear Research, Geneva, Switzerland
D. Fazioli‡, M. Breschi, University of Bologna, Bologna, Italy
M. Gast§, Karlsruhe Institute of Technology, Karlsruhe, Germany

Abstract

The development of a power converter for the resistive magnets of the Muon Collider Rapid Cycling Synchrotron (RCS) represents one of the most critical challenges of the muon accelerator system, given the required peak power levels in the 50–100 GW range. To address this, a modular resonant converter is proposed, consisting of several hundred identical series-connected cells interleaved with the magnets. This configuration distributes the total system voltage — on the order of tens of megavolts — evenly across the cells, while limiting the insulation voltage to ground. A key design requirement is a highly repeatable current ramp across successive pulses, with deviations at or below 100 ppm. Given the very short acceleration times, a pulse-to-pulse Iterative Learning Control (ILC) strategy is proposed to progressively meet this target. The paper presents the main converter topologies, repeatability studies, simulation results, and the proposed control approaches.

INTRODUCTION

The short muon lifetime necessitates extremely rapid acceleration across multiple Rapid Cycling Synchrotron (RCS) stages, with acceleration times of 0.5–6 ms and magnetic field ramp rates of 800–2000 T/s. To maximize muon survival and constrain RF peak power, acceleration must proceed in an approximately linear regime. The RCS geometry and magnet specifications [1] result in very large magnetic stored energy that must be delivered over very short intervals, implying peak power levels of 100 GW and operating voltages of 10 MV. Despite these extreme requirements, the low repetition rate of 5 Hz keeps the duty cycle very small, with current flowing for at most 6 ms per 200 ms cycle.

SWITCHED RESONANCE

In a previous paper [2], a resonant powering principle based on superimposed harmonics was proposed, where a main capacitor bank and an auxiliary series LC branch, connected in parallel, were simultaneously switched onto the magnet string to generate an approximately linear current ramp. This paper introduces a new concept, denoted as a switched resonant powering system, in which the converter is subdivided into hundreds of smaller series-connected power cells. Figure 1 shows the two possible single-cell topologies: unipolar (two-quadrant, allowing positive current and bipolar voltage) and bipolar (four-quadrant, allowing both current and voltage reversal). The bipolar configuration is required for the hybrid RCS (HCS), where part of the ring operates with a fixed dipole field and the remainder with a time-varying field. Tab. 1 lists the accelerator chains considered in the CERN (C) and GREENFIELD (GF) scenarios; simulation results presented here focus on the RCS1-C case.

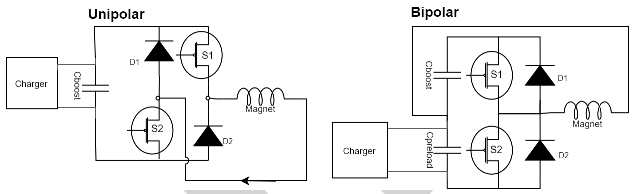

Figure 1: Unipolar and Bipolar switched resonance power cells.

Table 1: Accelerator Scenarios (U = Unipolar, B = Bipolar)

Scenario	E_{inj} [GeV]	E_{ext} [GeV]	Type	t_{ramp} [ms]	L_{tot} [m]
RCS1-C	63	350	U	0.45	4 103
RCS2-C	350	1 600	U	2.60	18 650
HCS3-C	1 600	3 800	B	4.42	12 940
RCS1-GF	63	314	U	0.35	3 654
HCS2-GF	314	750	B	1.10	2 539
HCS3-GF	750	1 500	B	2.37	4 366
HCS4-GF	1 500	5 000	B	6.37	20 376

In both power-cell topologies, the underlying operating principle is the same. A resonant interaction between the cell capacitor and the magnet string is established and terminated by periodically switching S_1 and S_2 between their ON and OFF states. A large number of such cells, potentially several hundred, can be connected in series and interleaved with the magnets, thereby forming a single series circuit, as schematically illustrated in Fig. 2. In this arrangement, the magnets do not require individual return-path extensions, except for the first and last units of the RCS. Since all magnet coils are connected in series and interleave with the power cells, the overall system behaves as a single electrical circuit, which avoids the need for independent current control of separate sectors.

RCS1 CERN Case Study

As a representative design exercise, the switched-resonance converter is dimensioned for the RCS1 CERN

* This work was supported by the European Union grant agreement 101094300 and is endorsed by the IMCC.
† fulvio.boattini@cern.ch
‡ davide.fazioli@studio.unibo.it
§ marco.gast15@gmail.com

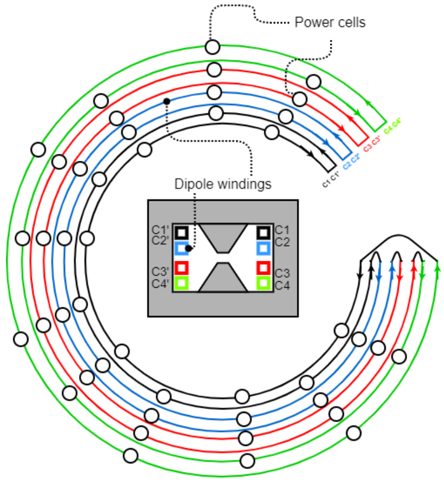

Figure 2: Dipole windings and power cells connection.

Table 2: RCS1 CERN Converter Parameters comparison

Parameter x_{grad}	1.02	1.20	1.40
Peak current I_{ext} [A]		11 674	
Ramp time t_{ramp} [ms]		0.45	
Capacitor voltage U_{C0}^{target} [kV]		10	
RMS magnet current I_{RMS} [A]	501	528	560
Capacitor energy per cell [kJ]	318	36	23
Total number of cells N_{cells}	885	1075	1286
Cabinet W × D=1.2 × H=2.5 [m]	3.50	1.90	1.80
Cost breakdown per cell [kAu]			
Semiconductor stacks	236	236	236
Capacitors	66.8	7.5	4.7
Charger	2.0	2.0	2.0
Cabinet	78.6	42.7	40.4
Total	**383**	**288**	**283**

scenario (Table 1), with magnets driven by a unipolar current ramp over 0.45 ms along 4103 m of resistive dipoles.

Using the POMARCS code suite (POwer and MAgnets for RCS, [3]), one can size magnets and power converters by specifying several parameters, including the gradient factor x_{grad}. This is the ratio of the peak instantaneous dI/dt of the resonant waveform to the average dI/dt of the corresponding linear ramp. For $x_{grad} = 1$, the ramp is perfectly linear; higher values increase the deviation from linearity, affecting power converter ratings and required peak RF power.

We compare $x_{grad} = \{1.02, 1.20, 1.40\}$ (Table 2). In each case, the number of total dipoles in the RCS is adjusted to keep the boost capacitor peak voltage near 10 kV, so N_{cells}, L_{cell}, and resistive losses per cell vary with x_{grad}. The same 4000 A / 6500 V IGBT/Diode press-pack is used in all three cases. As shown in Fig. 3, the capacitors are discharged more deeply as x_{grad} increases because the ramp becomes more sinusoidal. This reduces the installed capacitor energy at the cost of more cells and a higher total magnet voltage. The main electrical and cost parameters are given in Table 2.

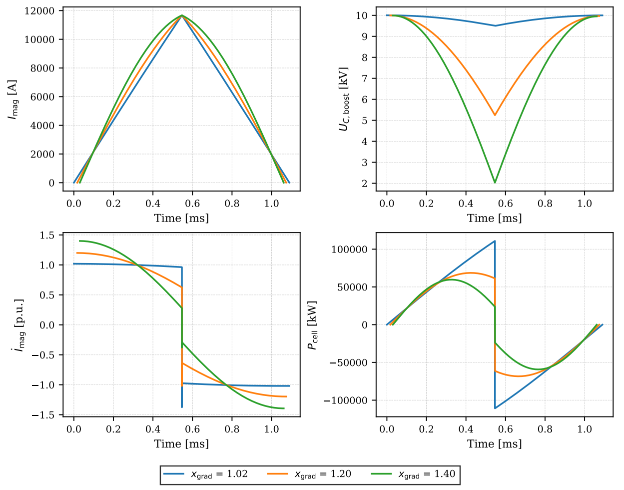

Figure 3: Comparison of three x_{grad} values (1.02, 1.20, 1.40). From top-left, clockwise: magnet current, boost capacitor voltage, instantaneous cell power, and normalised current derivative.

THE CONTROL PROBLEM

Active control of the current ramp is necessary for several reasons: the prescribed ramp shape must be reproduced with the required pulse-to-pulse repeatability, operating conditions may vary over time, and the relationship between winding current and magnetic flux density is not strictly linear due to magnetic saturation and eddy currents in the vacuum chamber.

The switching instants of S_1 and S_2 in each cell serve as control variables to shape the ramp. Given the short acceleration times, this control is implemented off-line via Iterative Learning Control (ILC), a technique well suited to systems repeatedly executing the same trajectory, as in an RCS. Once the appropriate switching pattern is identified, it remains fixed unless operating conditions change sufficiently to trigger a new learning transient. The achievable repeatability is ultimately bounded by the intrinsic repeatability of the system.

Intrinsic Repeatability

Repeatability is defined here as the statistical dispersion of nominally identical current ramps measured at the same time instants [4]. Let $I_i(t_j)$ be the current of the i-th ramp at discrete time t_j, over a set of N ramps. The mean current profile and the relative error of the i-th ramp with respect to the mean are defined as:

$$\bar{I}(t_j) = \frac{1}{N}\sum_{i=1}^{N} I_i(t_j), \qquad \varepsilon_i(t_j) = \frac{I_i(t_j) - \bar{I}(t_j)}{\bar{I}(t_j)} \quad (1)$$

The standard deviation of ε_i across all N ramps is computed at each time instant, and the worst-case time instant t^* is defined as the point where this spread is maximum:

$$\sigma(t_j) = \mathrm{std}_i[\varepsilon_i(t_j)], \qquad t^* : \sigma(t^*) = \max_{t_j} \sigma(t_j) \quad (2)$$

The intrinsic repeatability of the system is then characterised by $\sigma^* = \sigma(t^*)$. Assuming the relative errors follow a Gaussian distribution, approximately 95.4% of ramps will deviate from the mean by less than $\pm 2\sigma^*$ at any time instant. The design requirement is that this worst-case spread remains within ± 100 ppm:

$$2\,\sigma^* < 100 \text{ ppm} \tag{3}$$

This criterion is evaluated via a Monte Carlo study in which 1500 current ramps are simulated with IGBT firing delays drawn from a truncated Gaussian distribution. As shown in Fig. 4, increasing the number of cells reduces the worst-case spread through statistical averaging across independently jittering switches, confirming that the multi-cell architecture inherently satisfies the 100 ppm repeatability criterion.

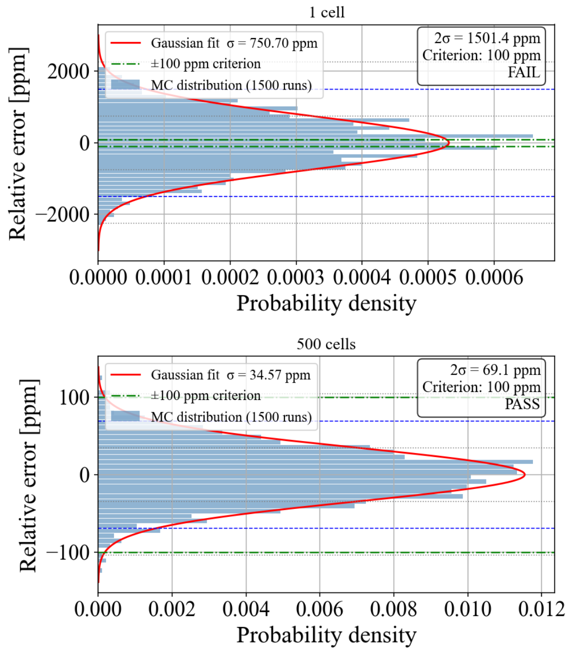

Figure 4: Worst-case relative current error distribution from 1500 Monte Carlo simulations of IGBT jitter: 1 cell (top) and 500 cells (bottom). The green dashed lines mark the ± 100 ppm criterion.

ILC Controller

ILC exploits the repetitive nature of RCS operation to correct the voltage reference pulse by pulse [5]. The general update law is:

$$u_{j+1}(k) = Q(q)\left[u_j(k) + L(q)e_j(k+1)\right] \tag{4}$$

where $Q(q)$ and $L(q)$ are the Q-filter and learning function. Adopting a PD-type algorithm:

$$u_{j+1}(k) = u_j(k) + k_p e_j(k+1) + k_d\left[e_j(k+1) - e_j(k)\right] \tag{5}$$

with $e_j(k) = I_{\text{ref}}(k) - I_j(k)$ and $u_{j+1}(k)$ is the voltage reference update for the power converter. Convergence is monitored via the mean relative tracking error:

$$J = \frac{1}{N}\sum_{k=1}^{N}\left|\frac{I_{\text{ref}}(k) - I_m(k)}{I_{\text{ref}}(k)}\right| \tag{6}$$

The algorithm is validated on an RK4-based pulse simulator of the RCS1-C scenario over 100 pulses. J decreases by more than two orders of magnitude before converging to a floor, as shown in Fig. 5. The bottom panel shows current tracking and per-cell capacitor voltages in the last iteration; capacitor voltages of the different power cells follow different discharge-recharge profiles according to when they are switched ON and OFF. This is the peculiar way the global modulator operates on the request of a given $V_{\text{ref},j+1}(k)$ profile.

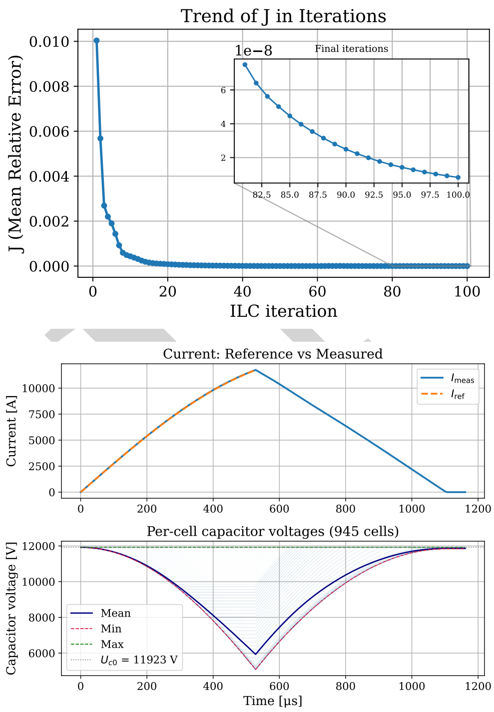

Figure 5: ILC simulation results for RCS1-C. Top: convergence of J over 5000 iterations (inset: zoom on final iterations). Bottom: last iteration — current tracking (top) and per-cell capacitor voltages (bottom).

CONCLUSION

A modular switched-resonance power converter for the Muon Collider RCS magnets has been presented and dimensioned for the RCS1-C scenario. The multi-cell series architecture distributes the tens-of-megavolt operating voltage across hundreds of cells, and the statistical averaging of independent IGBT jitter inherently meets the 100ppm repeatability requirement. Other factors, such as statistical dispersion of the charger voltage, may affect repeatability but are not analysed here. A PD-type ILC controller, validated over 100 simulated RCS1-C pulses, reduces the mean relative current error by more than two orders of magnitude, confirming the proposed control strategy's suitability for precision current-ramp tracking.

REFERENCES

[1] R. Taylor *et al.*, "Consolidated parameters", 2025. doi:10.5281/ZENODO.17476875

[2] D. Aguglia, F. Boattini, L. Bottura, and G. Brauchli, "A two harmonics circuit for the powering of the very fast RCS (Rapid Cycling Synchrotron) of the muon collider accelerator", in *Proc. IPAC'23*, Venice, Italy, pp. 3746–3749, Sep. 2023. doi:10.18429/JACoW-IPAC2023-WEPM078

[3] IMCC & MuCol Authors, POMARCS, 2025. https://gitlab.cern.ch/epc-hpc/muoncollider/pomarcs

[4] A. Dal Gobbo and D. Aguglia, "Global design analysis for highly repeatable solid-state klystron modulators", CERN, Geneva, CERN-ACC-2015-0008, 2015. https://cds.cern.ch/record/1981922

[5] DA. Bristow, M. Tharayil, and AG. Alleyne, "A survey of iterative learning control", *IEEE Control Systems Magazine*, vol. 26, no. 3, pp. 96–114, 2006. doi:10.1109/MCS.2006.1636313